POST MORTEM STUDY OF THE HEARTH CARBON REFRACTORIES OF TERNIUM BLAST FURNACE # 2[1]

Maria José Rimoldi[2]
Silvia camelli[2]
Adrián Vázquez[2]
Pablo Marinelli[3]
Enrique Doro[3]
Juan J. Mirabelli[3]

Abstract
After the blow-down of the Blast Furnace #2 of Termium Planta General Savio, there were taken 24 cores from different locations of the hearth in order to obtain samples from the different layers that formed the hearth's design. The scope of this work was to determine the wear profile of the hearth after eleven years of campaign and to identify the main wear mechanism of the refractory lining. The post mortem study included physical and mechanical properties determination, chemical composition analysis as well as crystalline phase identification by DRX and determination of the thermal conductivity at 400ºC. It was possible to determine the location of a brittle zone with presence of cracks, high apparent porosity and low mechanical strength. Among the wear mechanism, it was identified penetration of hot metal and alkalis, and the presence of circumferential and longitudinal cracks, responsible of the variation in the physical and mechanical properties of the carbon materials.
Key words: Blast furnace; Hearth; Refractory wear; Carbon

[1] *Technical contribution to the 3rd International Meeting on Ironmaking, September 22 – 26, 2008, São Luís City – Maranhão State – Brazil*
[2] *Materiales Refractarios, Instituto Argentino de Siderurgia, San Nicolás, Argentina.*
[3] *GMAT, Ternium Planta General Savio, San Nicolás, Argentina.*

1 INTRODUCTION

In an integrated steel mill, the blast furnace is the first link in the steel processing chain. Nowadays, blast furnace operational performance is measured through its productivity and fuel consumption. Modern blast furnaces have longer campaigns and operate at higher productivity levels, lowering costs and making the blast furnace / BOF route competitive.
The hearth refractory is a critical area of the blast furnace. It is difficult to repair and the blast furnace campaign depends on the hearth life. The detection or monitoring of the hearth wear is the key to understanding wear process and protecting the blast furnace hearth.(1) Studies revealed that elephant foot type wear and the presence of embrittlement refractory zone were serious threats to campaign life.(2)
Several useful technologies had been developed to detect and monitor the hearth wear. The main methods can be classified in two types: heat transfer analysis and measurement and acoustic measurement.
Ternium Siderar Blast furnace # 2 had its start up in September 1995. After 11-year operation, in October 2006, the blast furnace was blown out to relining. During this campaign it produced 22,7 millions tones.(3)
The objective of this work was to analyze the wear mechanism of the hearth refractory lining of Ternium Siderar Blast furnace # 2. Also, the hearth wear profile was determined and this profile was compared with acoustic technique and hearth bottom temperatures model control.
Hearth refractory lining post mortem study was performed through physical and mechanical properties determination, chemical composition analysis as well as crystalline phase identification by XRD.

2 MATERIALS AND METHODS

The samples were obtained by core drilling before and during the hearth demolition. In figure 1 is shown the equipment used in the core drilling.
The Blast Furnace # 2 hearth design is presented in figure 2. It consists of a layer of semi graphite BC-30 bricks, 3 layers of carbon BC-7S bricks, a layer of Alumina-SiC and one layer of high fired super duty bricks in the bottom; carbon BC-5 in the hearth walls. The hearth diameter was 10,4 m.(4)
Twenty four samples were taken from the blast furnace hearth and bottom after the blow out. The detailed locations of the core samples are presented in figure 3. The samples were drilled between the middle of layer 3 and layer 11. Table 1 summarizes core samples colleted from blast furnace hearth at different heights.

Figure 1. Equipment used to hearth core drilling.

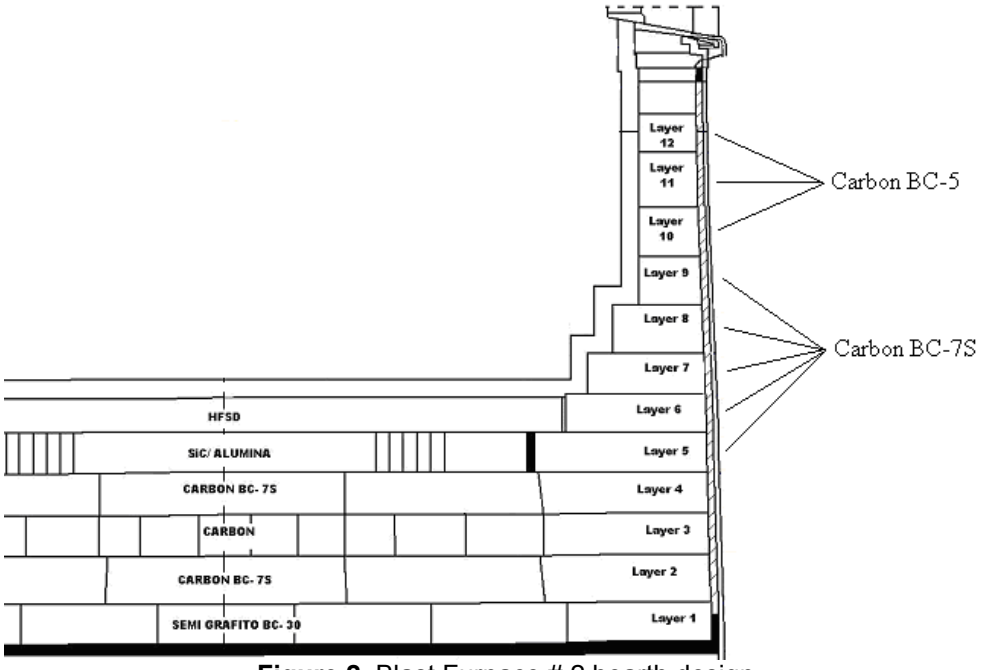

Figure 2. Blast Furnace # 2 hearth design

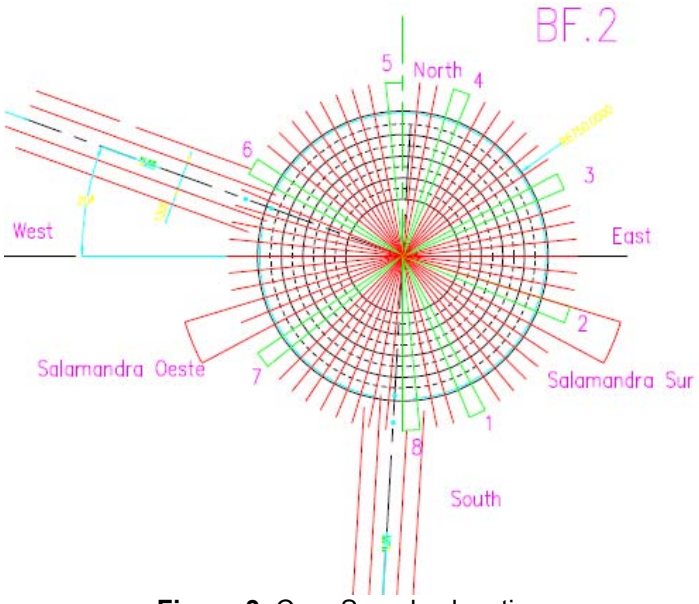

Figure 3. Core Samples locations.

Table 1. Core samples colleted from blast furnace heath

Layer	Height (m)	Location							
		1	2	3	4	5	6	7	8
L3	1050		**X**				**X**	**X**	**X**
L4	1551	**X**	**X**		**X**		**X**		
L5	2053	**X**	**X**				**X**	**X**	
L6	2555		**X**				**X**		
L7	3057				**X**				
L8	3608		**X**			**X**			
L9	4208							**X**	
L10	4609		**X**						
L11	5210							**X**	

The following characterization techniques were employed in this study:

- Chemical analysis (X-ray fluorescence)
- Weight loss
- Bulk density and apparent porosity
- X-ray diffraction
- Cold crushing strength
- Thermal conductivity at 400ºC

3 RESULTS

The core sample took from layer 4 – location 1 is shown in Figure 4. The core was about 1500 mm long and consisted of three zones: carbon without visual alteration (900 mm), cracked carbon and skull. The cracked carbon presented different colorations and circumferential and horizontals cracks; also was found to be impregnated with iron (Figure 5).

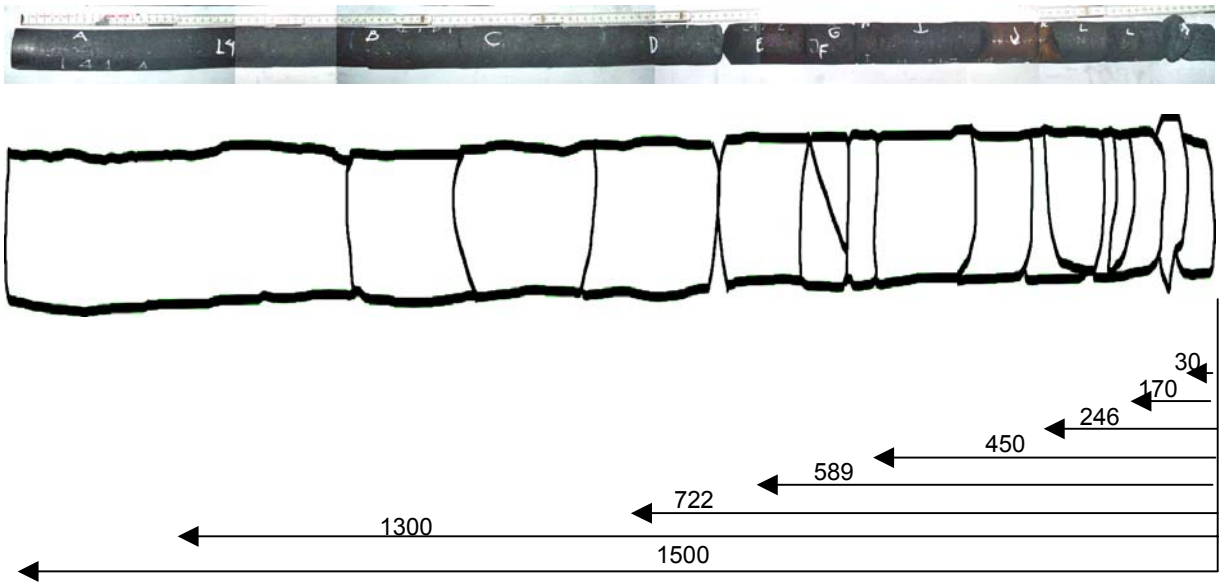

Figure 4.Core sample: layer 4 - location 1

Figure 5.Cracked carbon: 500 mm.

Physical properties and chemical analyses were tested at different distance from the hot surface (Tables 2 and 3)

Table 2. Bulk density and apparent porosity at different distances from the hot face of the core sample layer 4 – location 1.

Distance from the hot face (mm)	Bulk density (g/cm^3)	Apparent porosity (%)
246	4,75	10,4
500	1,88	11,8
589	1,88	12,2
722	1,62	16,6
1300	1,60	17,6

Table 3. Chemical composition, at different distances from the hot face, of the core sample layer 4 – location 1.

Distance form the hot face (mm)	30	170	246	450	500	589	722	1300
Al_2O_3 (%)	3,4	3,2	3,0	4,0	4,1	4,2	3,3	3,5
SiO_2 (%)	13,9	12,9	17,4	14,3	13,9	13,9	13,2	14,1
Fe_2O_3 (%)	0,4	0,5	77,9	10,7	11,5	11,4	0,4	0,6
TiO_2 (%)	0,1	-	0,4	-	0,1	0,04	-	-
K_2O (%)	0,1	0,1	0,1	0,2	0,2	0,12	0,1	0,3
Na_2O (%)	0,1	-	-	-	0,1	-	0,1	0,1
CaO (%)	0,1	0,1	0,1	0,1	0,1	0,1	0,1	0,1
Wight Loss (%)	81,8	83,1	0,2	70,3	69,7	69,7	82,7	81,2

The X-ray diffraction results for the core samples at different distances from the hot face are shown in Table 4.

Table 4. XRD analyses of the core sample layer 4 – location 1.

Distance from the hot face (mm)	Crystalline phases
500	• Graphite (C) • Corundum (Al_2O_3) • Tridimitte (SiO_2)
722	• Graphite (C) • Corundum (Al_2O_3) • Silicon Carbide (SiC)
1300	• Graphite (C) • Corundum (Al_2O_3) • Silicon Carbide (SiC

The core sample took from layer 5 – position 1 is shown in Figure 6. The core was about 1730 mm long and consisted of three zones: carbon without visual alteration (620 mm), cracked carbon and skull. The cracked carbon was found to be impregnated with iron (Figure 7).

Physical properties and chemical analysis were tested at different distance from the hot surface (Tables 5 and 6). The crystalline phases identified by XRD are presented in Table 7.

The thermal conductivity for the carbon cold face, at 1500 mm from the hot surface, was 12 W/mK at 400 ºC.

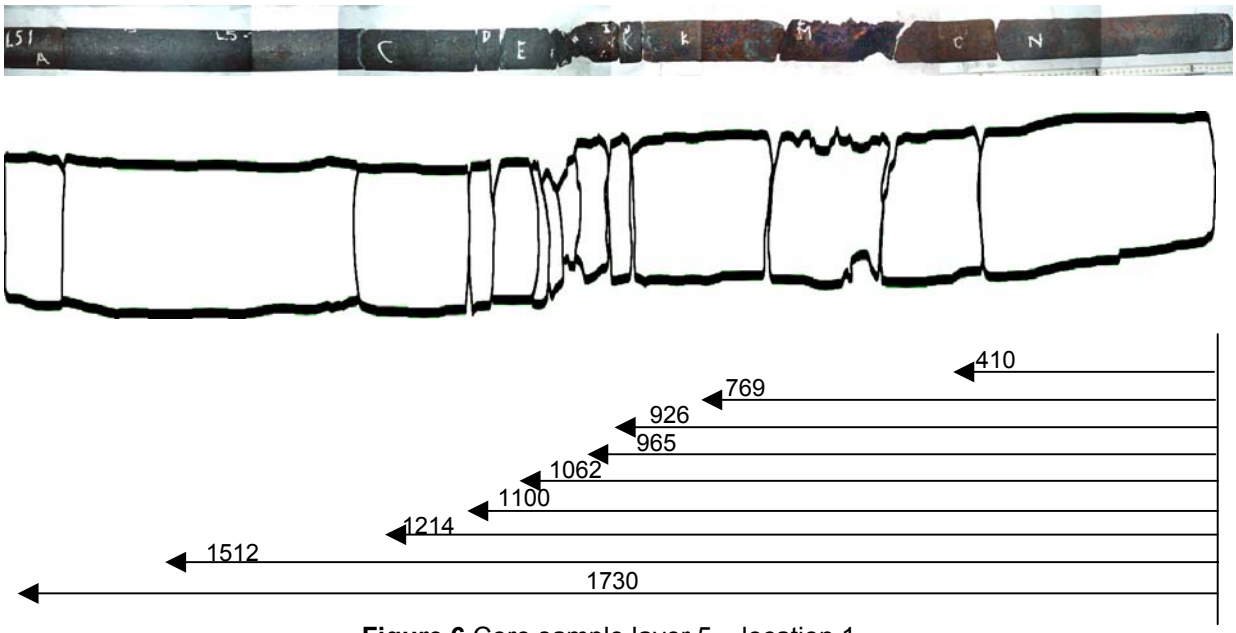

Figure 6.Core sample layer 5 – location 1

Figure 7.Craked carbon impregnated with iron

Table 5. Bulk density and apparent porosity of the cores sample: layer 5 – location 1.

Distance from the hot face (mm)	Bulk density (g/cm^3)	Apparent porosity (%)
867	1,80	16,3
926	1,70	17,2
1110	1,55	21,5
1512	1,62	16,1

Table 6. Chemical composition of the core sample layer 5 – location 1.

Distance form the hot face (mm)	410	769	926	965	1110	1214	1512
Al_2O_3 (%)	3,7	1,8	4,6	5,3	3,3	3,4	3,2
SiO_2 (%)	7,7	4,2	16,2	13,8	14,1	13,8	12,4
Fe_2O_3 (%)	20,3	61,4	5,8	14,8	0,5	0,7	0,5
TiO_2 (%)	-	-	0,1	0,04	0,04	0,1	0,1
K_2O (%)	0,6	0,3	0,1	2,1	0,2	0,3	0,1
Na_2O (%)	-	-	0,1	0,6	0,1	0,2	-
CaO (%)	28,0	12,2	0,1	0,1	0,1	0,2	0,1
Wight Loss (%)	1,7	1,1	82,7	62,8	81,5	81,4	83,5

Table 7. XRD analyses of the core sample layer 5 – location 1.

Distance from the hot face (mm)	Crystalline phases
926	• Graphite (C) • Magnetite (Fe_3O_4) • Iron (Fe)
1062	• Graphite (C) • Corundum (Al_2O_3) • Silicon Carbide (SiC)
1512	• Graphite (C)

The horizontal core sample took from layer 3 – position 2 is shown in Figure 8. The core was about 1650 mm long and consisted of carbon without visual alteration (1500 mm) and carbon with iron contamination (140 mm). The physical properties and chemical analysis were tested at different distance from the hot surface (Tables 8 and 9).

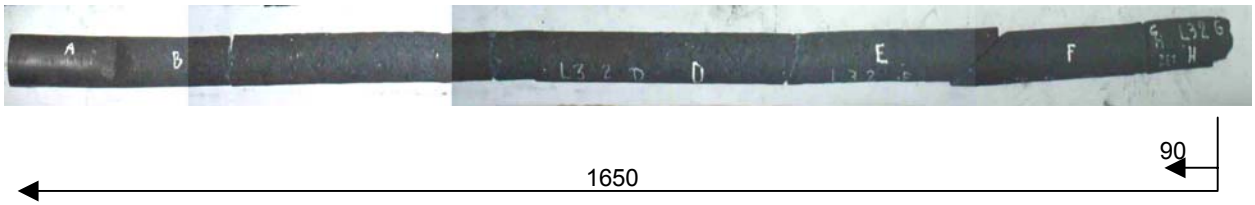

Figure 8.Core sample: layer 3 – location 2

Table 8. Bulk density and apparent porosity at different distances form the hot face of the sample Layer 3 – Location 2.

Distance from the hot face (mm)	Bulk density (g/cm^3)	Apparent porosity (%)
50	1,67	11,2
92	1,66	13,1

Table 9. Chemical composition, at different distances from the hot face, of the core sample layer 3 – location 2.

Distance form the hot face (mm)	50	92
Al_2O_3 (%)	3,3	3,2
SiO_2 (%)	13,7	13,9
Fe_2O_3 (%)	0,5	0,3
K_2O (%)	0,2	0,1
CaO (%)	0,1	0,1
Wight Loss (%)	82,1	82,2

The core sample took from layer 4 – position 4 is shown in Figure 9. The core was about 1110 mm long and consisted of carbon without visual alteration (950 mm) and carbon with micro cracks (130 mm). The chemical analysis was tested at different distance from the hot surface (Table 10).

Figure 9.Core sample: layer 4 – location 4.

Table 10. Chemical composition, at different distances from the hot face, of the core sample layer 4 – location 4.

Distance form the hot face (mm)	**481**	**786**	**961**
Al_2O_3 (%)	3,3	3,4	3,4
SiO_2 (%)	13,5	13,8	13,1
Fe_2O_3 (%)	0,4	0,4	0,3
TiO_2 (%)	-	-	-
K_2O (%)	0,2	0,1	0,1
Na_2O (%)	-	-	-
CaO (%)	0,1	0,1	0,1
Wight Loss (%)	82,3	82,0	82,9

Cold crushing strength of core samples at different distances from the hot face is presented in Table 11.

Table 11. Cold crushing strength of different post mortem samples.

Layer	**Location**	**Distance from the hot face (mm)**	**Cold crushing strength (MPa)**
4	1	1300	35
3	2	160	36
4	4	192	26
		481	27
		786	28
		961	39

The vertical core sample took from the hearth bottom corresponding to layer 3 is shown in Figure 10. The core was about 430 mm long; the chemical analysis and the physical properties were tested at different distance from the hot surface (Tables 12 and 13).

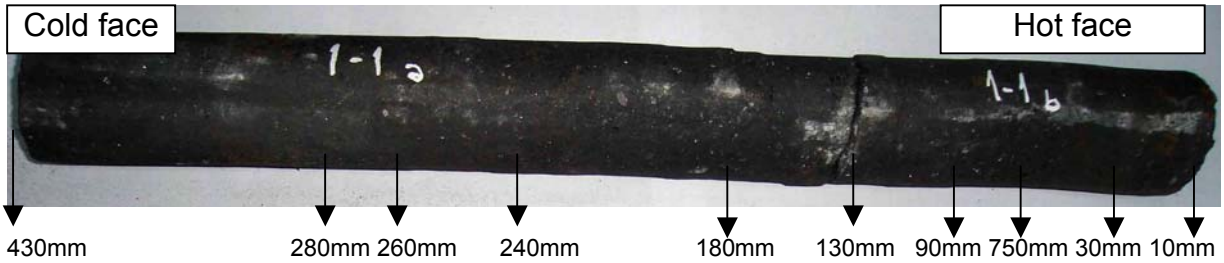

Figure 10. Core sample: layer 3 – hearth bottom

Table 12. Chemical composition, at different distances from the hot face, of a sample taken from the hearth bottom.

Distance form the hot face (mm)	<10	30	75	90	130	240	260	280	430
Al_2O_3 (%)	4,5	8,4	4,4	8,6	3,8	6,0	4,0	5,4	3,2
SiO_2 (%)	11,3	29,0	15,5	33,3	13,6	23,4	14,8	21,6	13,2
Fe_2O_3 (%)	28,0	19,4	4,3	3,6	1,7	4,4	4,0	8,8	0,6
TiO_2 (%)	0,1	0,2	0,08	0,2	0,1	0,1	0,1	0,1	0,1
K_2O (%)	1,2	0,4	0,13	0,4	0,1	0,2	0,1	0,2	0,2
Na_2O (%)	0,3	0,3	-	-	-	-	-	-	-
CaO (%)	0,5	0,4	0,12	0,5	0,1	0,3	0,1	0,3	0,2
Wight Loss (%)	53,9	41,2	75,3	52,6	80,4	65,3	76,7	63,3	82,3

Table 13. Bulk density and apparent porosity at different distances form the hot face of the post mortem sample taken form the hearth bottom - Layer 3.

Distance from the hot face (mm)	Bulk density (g/cm^3)	Apparent porosity (%)
< 10	2,43	10,8
30	1,87	9,0
75	1,76	9,2
130	1,75	9,4
180	1,73	9,1
240	1,76	8,9
280	1,85	8,8
430	1,71	10,6

4 DISCUSSION

The hearth wear profile determined by core sample and the theoretical wear profile determined by the position of the hot metal solidification isotherm (1150ºC isotherm) is shown in Figure 11. Also, in this figure the theoretical wear profile estimated by acoustic measurement is presented.

The 1150ºC isotherm represents the penetration limit of hot metal into the carbon refractory material.[4]

The weight loss at different distances from the hot face of the cores sample layer 4 locations 1 is presented in figure 12. At 250 mm from the hot face there was identified a hot metal skull, corresponding to a high- density zone (Figure 13).

The alkali content remained almost constant in core sample taken from layer 4 – location 1.

In the core sample layer 5 – location 1, alkali content was 2,7% at 965 mm from the hot face (Figure 14). This zone presented cracks and powdered material. The brittle zone was identified between 950 mm and 1100 mm from the hot surface. In this zone, the apparent porosity was the highest measure obtained. The iron penetration reached until the beginning of the brittle zone.

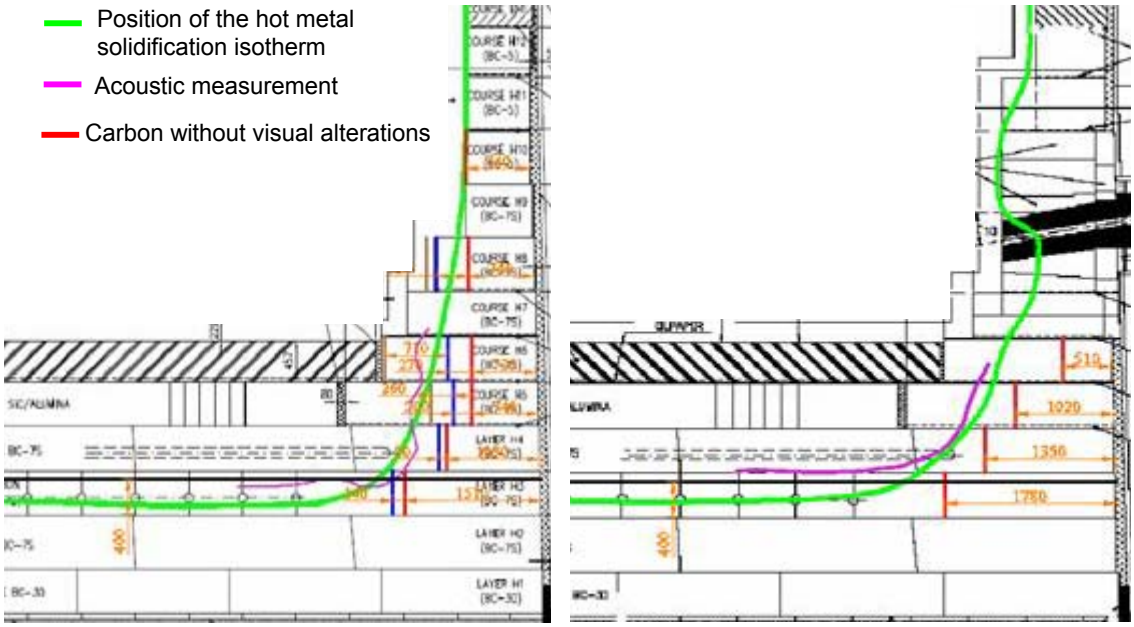

(a) Location 2 (b) Location 6

Figure 11. Heart wear profile: core drilling, predicted by acoustic measurement and the 1150ºC isotherm position.

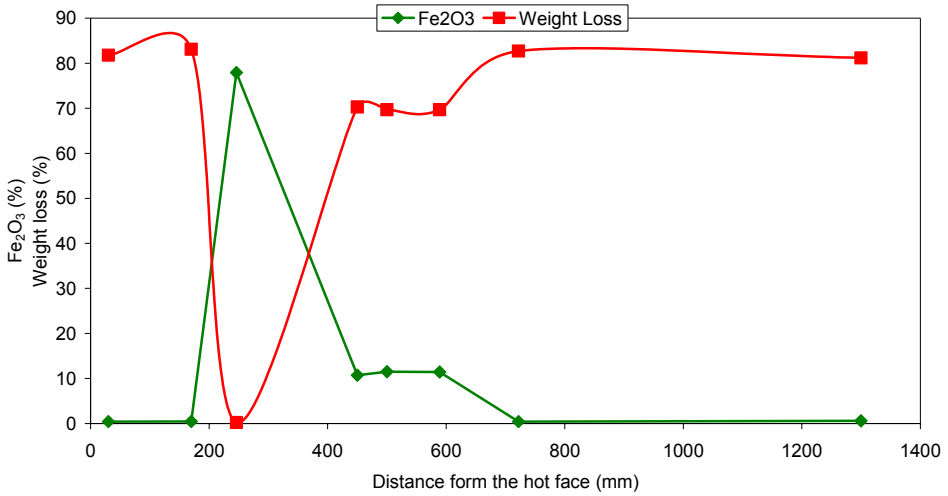

Figure 12. Evolution of the weight loss and iron content of the core sample layer 4 location 1.

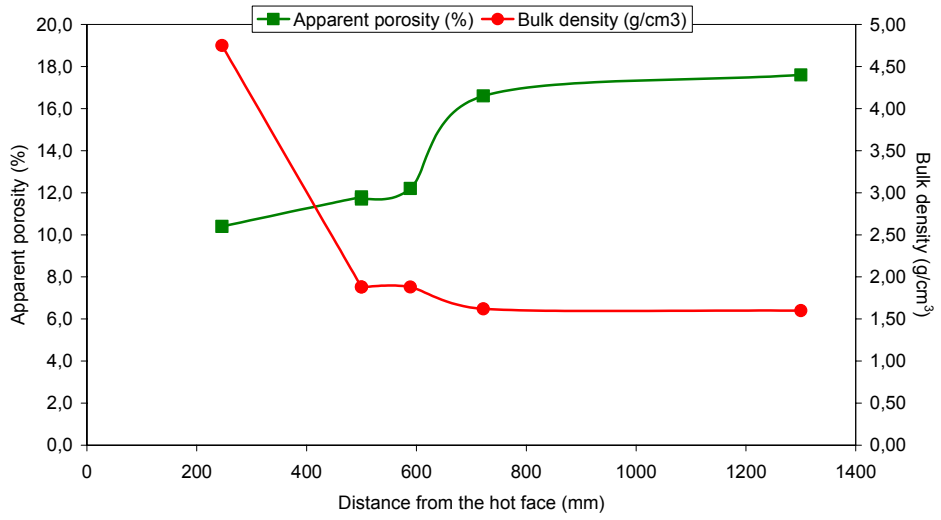

Figure 13. Evolution of the physical properties of the core sample layer 4 location 1.

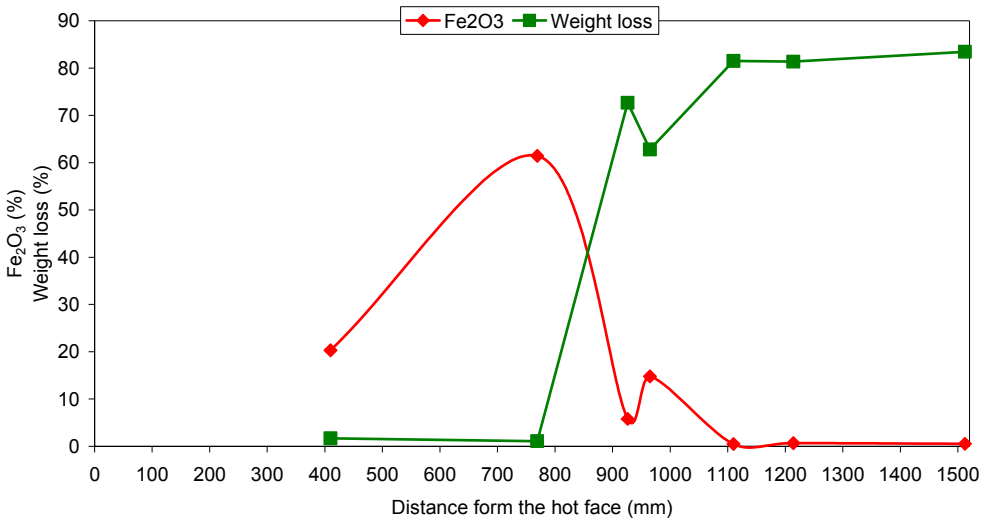

Figure 14. Evolution of the weight loss and Fe and alkali content of the core sample layer 4 location 1.

From the technical sheet, the thermal conductivity at 400ºC is 13,5 W/mK, the bulk density is 1,62 g/cm^3 and the cold crushing strength us 44 MPa. These properties evaluated in the cold face of the core samples were in the typical range.

5 CONCLUSION

In the hearth walls, the real wear profile of the refractory lining was higher than of the predicted profile. Only layers 8 and 9 maintained the original thickness (740 mm).
The carbon material in the cold face of the hearth wall presented physical, mechanical and thermal properties similar to the unused BC7-S carbon blocks. The thickness of unaltered zone varied between 620 mm to 950 mm.
The brittle zone was detected at 950 mm from the hot face of the wall. This zone presented cracks, powdered material and high alkali content as well as alteration in its physical properties.
The bottom of the hearth (layer 3) presented a 20-percent reduction in its thickness. In this layer, the densification of the hot face was due to the high iron content and alkali diffusion. Nevertheless, the iron was present in the entire core sample.
The main wear mechanisms of the refractory lining of the hearth were erosion/ abrasion and chemical corrosion by hot metal penetration and alkali diffusion.

REFERENCES

1 HUANG, D., CHAUBAL, P., ABRAMOWITZ, H., ZHOU, C. Hearth skulls and hearth wear investigation of ISPAT Inland's #7 blast furnace. In: AISTech 2005 Proceedings, V I, 2005. p 101-112.
2 FRASER, B., CUMMINS, J., BROWN, G., DWIGHT, R. In-service performance of micropore carbon at Newscatle BF 3. In: AISTech 2004 Proceedings, V I, 2004. p 57-66.
3 LINGIARDI, O., MUSANTE, R., VELO, E., AMETRANO, R., ZUBIMNEDI, J., GÓMEZ, O. DE NICOLA, H. Ternium-Siderar Blast Furnace #2: end of campaign. In: AISTech 2007 Proceedings, 2007.
4 LINGIARDI, O., ZUBIMNEDI, J., AMETRANO, R., GIANDOMENICO, F., GONZALEZ, N. Hearth wearing in Siderar Blast Furnace Nº2. In: 2nd International Meeting on Ironmaking, 2004, Vitória, São Paulo, ABM. P 213-225.